Degenerative changes are associated with severity of anterior cruciate ligament injury within the skeletally immature joint

Danielle Howe[1,2], Jacob D. Thompson[1,2], Stephanie D. Teeter[1], Olivia Barlow[3], Emily H. Griffith[4], Lauren V. Schnabel[2,5], Jeffrey T. Spang[6], Matthew B. Fisher[1,2,6*]

Affiliations:

[1]Joint Department of Biomedical Engineering, North Carolina State University and the University of North Carolina at Chapel Hill; Raleigh, NC, 27695, USA

[2]Comparative Medicine Institute, North Carolina State University; Raleigh, NC, 27607, USA

[3]Department of Mechanical Engineering, North Carolina State University; Raleigh, NC, 27607, USA

[4]Department of Statistics, North Carolina State University; Raleigh, NC 27695

[5]Department of Clinical Sciences, North Carolina State University; Raleigh, NC, 27695, USA

[6]Department of Orthopaedics, University of North Carolina at Chapel Hill; Chapel Hill, NC, 27599, USA

*Corresponding author. Email: mbfisher@ncsu.edu

Abstract

Anterior cruciate ligament (ACL) injuries are a major problem in the pediatric and adolescent populations. Approximately one-quarter of these injuries extend through only part of the tissue cross-section. Yet, there is very limited data to inform clinical treatment for pediatric partial ACL tears. In particular, it is unknown how injury severity impacts long-term degenerative changes in the joint. In this study, we leverage a skeletally immature preclinical porcine model to evaluate joint biomechanics, tissue remodeling, and degeneration after partial (isolated anteromedial (AM) or posterolateral (PL) bundle) or complete (full thickness) ACL injury. Six months after injury, joint laxity increases were minimal for PL bundle injury, minor for AM bundle injury, and major for ACL injury. In both partial injury cases, the remaining bundle remodeled through an increase in cross-sectional area to attempt to restore ACL function and stabilize the knee joint. Joint degeneration (evaluated by cartilage T1 relaxation, macroscopic cartilage degeneration, and meniscal hypertrophy) was minimal after PL bundle injury, moderate after AM bundle injury, and substantial after ACL injury. The findings for partial injury were further substantiated in an older cohort of adolescent animals. Further analysis with subjects grouped by Lachman grade (indicating the extent of joint destabilization) indicated that degeneration was associated with the extent of biomechanical destabilization, irrespective of the injury type. These findings point to the importance of considering the results of joint laxity when creating treatment plans for young patients with significant growth remaining, particularly those with partial ACL injuries.

INTRODUCTION

Injuries to the anterior cruciate ligament (ACL) of the knee, particularly those occurring in children and adolescents, are a significant clinical and societal concern (*1*). While the total number of ACL injuries across all age groups is substantial (200,000-250,000 yearly in the United States alone) (*2, 3*), a specific concern is the 2-4 times increase in the rate of injury and subsequent surgical treatment in the pediatric population compared to adults (*4-6*). In the pediatric population, full-thickness ACL tears result in two-fold increases in knee laxity (*7*) and 3-4 times greater risk of developing meniscal and cartilage lesions with delayed surgical intervention (*8*). As a result, surgical reconstruction is the standard practice to restore joint stability for young, active patients with complete ACL tears (*9*), despite some concern over growth plate disruption. However, for partial-thickness ACL tears, which account for approximately 25% of diagnosed ACL injuries (*10*) and result in a more minor (~30% on average) increase in knee laxity (*11*), the choice of operative or non-operative treatment is less evidence-based. Preventing degeneration is a major concern. On one hand, the current lack of data on partial ACL injuries in the pediatric population may lead to non-surgical treatment in cases where surgery is actually needed to limit degenerative changes (*13*). Supporting this notion, subsequent meniscal and chondral pathologies after non-surgical treatment of partial tears are reported in young patients, with a similar incidence compared to reports in patients with full thickness tears after ACL reconstruction (*14*). On the other hand, unnecessary surgeries can exacerbate degenerative changes (*12*). Approximately 50% of young patients who undergo ACL reconstruction develop osteoarthritis after 10 years (*15*), leaving a growing population of patients aged 20-30 years decades away from eligibility for a knee replacement with few treatment options.

64 A major complicating factor in determining the best clinical treatment is that not all
65 partial tears and not all patients are the same. The ACL has two major subregions, the
66 anteromedial (AM) bundle and the posterolateral (PL) bundle, and partial tears can occur in
67 either. Tear location may impact functional outcomes after partial injury, and the results may
68 differ between children and adults. Specifically, a study in adult patients reported similar joint
69 stability after isolated AM and PL bundle injuries (*11*), while a study in pediatric patients
70 reported better outcomes for AM bundle injuries (*16*). Furthermore, in a skeletally immature pig
71 model, the biomechanical function of the AM and PL bundles of the ACL depends on age and
72 sex, such that the AM bundle plays a larger functional role in older versus younger subjects and
73 males compared to females (*17, 18*). Since evidence regarding treatment of bundle-specific
74 partial injuries in children and adolescents is sparse, there is a need for further investigation of
75 long-term outcomes and degenerative changes in skeletally immature subjects. Large exploratory
76 studies in humans are challenging to perform in the pediatric patient population. However, the
77 pig is a valuable preclinical model with similar ACL anatomy and function to humans (*19-21*),
78 which can be used to control injury severity and assess functional outcomes and degenerative
79 changes after injury.
80 In the present study, we investigated biomechanics, remodeling, and degeneration in the
81 knee joint after isolated AM bundle, PL bundle, and complete ACL tears in a juvenile porcine
82 model. We hypothesized firstly that partial (AM and PL bundle) tears would result in small
83 levels of instability and degeneration, which would be less severe compared to complete ACL
84 tears. Secondly, we hypothesized that remaining soft tissues in the joint would remodel in
85 response to changes in biomechanical loading after ACL injury, corresponding to the injury
86 severity. At 6 months after injury, joint laxity showed no change after PL bundle injury, minor

87 increases after AM bundle injury and major increases after ACL injury. Similarly, PL bundle
88 injury resulted in minimal degeneration, AM bundle injury resulted in moderate degeneration,
89 and complete ACL injury led to substantial degeneration, such that the degree of degenerative
90 changes was associated with joint instability.
91

92 **RESULTS**

93 **Joint kinematics after partial and complete ACL Injury**

94 To evaluate the impact of AM and PL bundle tears on knee function and degeneration in
95 skeletally immature subjects, we performed arthroscopic transection and removal of the AM
96 bundle (AM-), PL bundle (PL-) or ACL (ACL-) in juvenile Yorkshire crossbreed pigs, and
97 assessed biomechanics and joint health after 24 weeks (Fig. 1A). A sham operation was
98 performed in contralateral joints. Joint kinematics were evaluated using a robotic testing system
99 first under applied anterior-posterior (AP) drawer to simulate clinical exams (Fig. 1B). Force-
100 translation curves from PL- joints were nearly indistinguishable from sham-operated controls,
101 while curves from AM- joints extended further in the anterior direction, and curves from ACL-
102 joints extended far beyond the others (Fig. 1C). AP tibial translation (APTT) was greater in AM-
103 joints (46%, $P<0.0001$) and ACL- joints (195%, $P<0.0001$) compared to contralateral controls,
104 while PL- joints showed no significant difference ($P=0.22$) (Fig. 1D). Between injury groups, the
105 inter-limb difference in APTT was significantly different for all comparisons ($P\leq0.0061$) (Fig.
106 1E). Under applied compression (Fig. 1F-I) (to simulate weight bearing) and varus-valgus
107 moments (Fig. 1J-M) (to simulate rotational loads), differences between force-translation curves
108 for PL- and AM- joints were less striking (though still present), but curves for ACL- joints
109 remained distinct. Under compression, anterior tibial translation (ATT) was only greater in ACL-

joints compared to contralateral controls (327%, P=0.0005) (Fig. 1H), and the interlimb difference in ATT was greater for the ACL- group compared to AM- and PL- groups (P<0.0001 for each) (Fig. 1I). Likewise, varus-valgus (VV) rotation was greater in ACL- joints compared to contralateral controls (33%, P=0.012) (Fig. 1L), with a larger interlimb difference compared to AM- and PL- groups (P≤0.0037) (Fig. 1M). Sex did not significantly affect kinematics under AP or VV loads, but under compression, ATT was significantly greater in males than females within the AM- group (P=0.003) (Fig. S1). Overall, PL bundle injury induced minimal joint instability, AM bundle injury induced moderate joint instability, and complete ACL injury induced major joint instability.

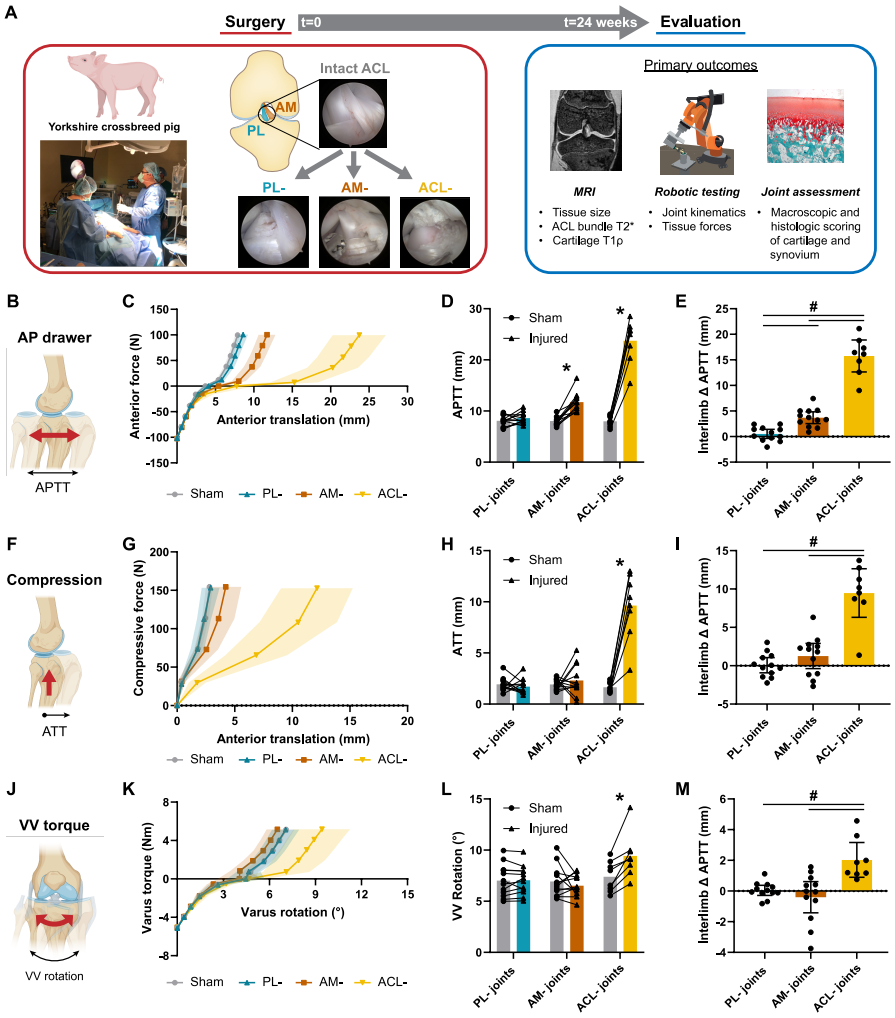

120 **Fig. 1. Biomechanical assessment of porcine joints 6 months after partial and complete**
121 **ACL transection.** (A) Schematic of arthroscopic transection of the AM bundle, PL bundle, or
122 entire ACL, followed by evaluation after 24 weeks. (B) Diagram of anterior-posterior (AP) loads
123 applied to the tibia. (C) Resulting mean force-translation curves. AP tibial translation (APTT)
124 shown as (D) absolute values and (E) interlimb differences. (F) Diagram of compressive load
125 applied to the tibia. (G) Resulting mean force-translation curves. Anterior tibial translation
126 (ATT) shown as (H) absolute values and (I) interlimb differences. (J) Diagram of varus-valgus
127 (VV) torques applied to the tibia. (K) Resulting mean torque-rotation curves. VV rotation shown
128 as (L) absolute values and (M) interlimb differences. Red arrows indicate the direction of the
129 applied load, and black arrows indicate the direction of measured translation (B, F, J). Points and
130 shaded area represent mean ± 95% CI (C, G, K). Lines connect paired joints (D, H, L).
131 Individual data points (n=12 for PL- and AM- groups, n=8 for ACL- group) presented with mean
132 ± 95% CI (E, I, M). * $P<0.05$ between injured and contralateral, from paired t-test with Holm-
133 Sidak correction. #$P<0.05$ between injury type, from one-way ANOVA with Tukey post hoc test.
134

135 **Remodeling of the uninjured bundle of the ACL**

136 In partial injury (AM- and PL-) joints, the in-situ force (Fig. 2A) carried by the remaining
137 ACL bundle was greater compared to the corresponding bundle force in contralateral controls
138 under applied anterior drawer ($P\leq0.00019$ for both injury types) (Fig. 2B). However, under joint
139 compression, the remaining bundle force was elevated only for AM- joints ($P=0.0016$) (Fig. 2C).
140 Remaining bundle in-situ force did not differ on average under varus or valgus moments,
141 although considerable specimen-to-specimen variability existed (Fig. S2). To assess structural
142 remodeling of the ACL that may drive functional changes, the cross-sectional area (CSA) of the

remaining bundle in injured joints was measured from MRI and compared to the corresponding bundle in contralateral joints (Fig. 2D). The remaining bundle was larger in CSA compared to contralateral controls for PL- joints (AM bundle) by 13% and AM- joints (PL bundle) by 60% ($P \leq 0.022$, for both) (Fig. 2E). In addition, bundle collagen organization was assessed through T2* mapping using MRI (Fig. 2F), and no differences were found in median T2* value of the remaining bundle in injured joints compared to the corresponding bundle in contralateral joints for either injury group (Fig. 2G). These data indicate that after partial ACL injury, the remaining bundle adjusted to loss of function of the injured bundle by increasing in functional load contribution and CSA while maintaining tissue quality (inferred from T2* values) compared to contralateral controls.

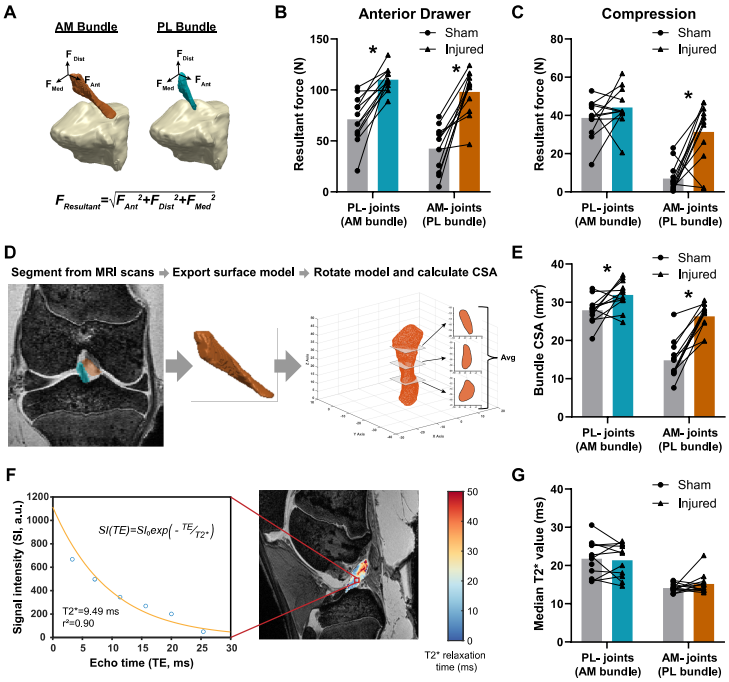

Fig. 2. Remodeling of the remaining bundle after transection of the AM or PL bundle of the ACL. (A) In-situ bundle forces measured under applied loads. Resultant force in the uninjured bundle under applied (B) anterior drawer and (C) compression. (D) Schematic demonstrating methods used to measure bundle cross-sectional area (CSA) from segmented MRI scans. (E)

158 CSA of the uninjured bundle. (F) Schematic showing representative sagittal MR image overlaid
159 with the T2* map of the ACL. Plot shows signal intensity at the six measured echo times (blue
160 circles) and fitted monoexponential decay curve (yellow) for a representative voxel. Calculated
161 T2* relaxation time and goodness-of-fit (r^2) shown in graph. (G) Median T2* value of the
162 uninjured bundle. Lines connect paired joints. *P<0.05 between injured and contralateral, from
163 paired t-test with Holm-Sidak correction. Individual data points (n=12 per injury group)
164 presented with mean/median.
165

166 **Cartilage and Synovium Degeneration**

167 To assess if the type of injury impacted degeneration of articular cartilage in the joint,
168 T1ρ mapping was performed via MRI, and the median T1ρ value was calculated for the medial
169 and lateral femoral and tibial articular cartilage (Fig. 3A). Higher T1ρ values are linked to lower
170 proteoglycan content (*22, 23).* Qualitatively, average side-to-side differences in T1ρ values
171 relative to the contralateral control were smallest in PL- joints and largest in ACL- joints, with
172 AM- joints falling in between for all regions (Fig. 3B-E). Statistically, T1ρ values relative to the
173 contralateral control were not significantly elevated in any compartment for the PL- group, but
174 were elevated in the medial femoral and lateral tibial compartments for the AM- group and the
175 lateral femoral and lateral tibial compartments for the ACL- group (P≤0.022 for all, Fig. 3B-E).
176 Furthermore, the interlimb difference in T1ρ values were significantly greater in the AM- group
177 relative to the PL- group for the medial femoral compartment and in the ACL- group relative to
178 the PL- group for the lateral femoral and lateral tibial compartments (P≤0.012 for all).
179 Macroscopic articular cartilage damage was scored from 0 to 4 according to Osteoarthritis
180 Research Society International (OARSI) guidelines *(24*) for the four compartments (Fig. 3F, Fig.

S3) and summed for a composite joint score. The composite joint scores were significantly elevated compared to contralateral controls for only the ACL- group (P=0.016 Fig. 3G). Synovium pathology was similarly evaluated through macroscopic scoring, though no significant differences were found in synovium scores between groups (Fig. 3H). Overall, minimal cartilage degradation was observed in PL- joints, and similar increases in cartilage T1ρ values (an early indicator of cartilage degradation) were observed in AM- and ACL- joints; however, macroscopic cartilage degeneration was elevated only in ACL- joints.

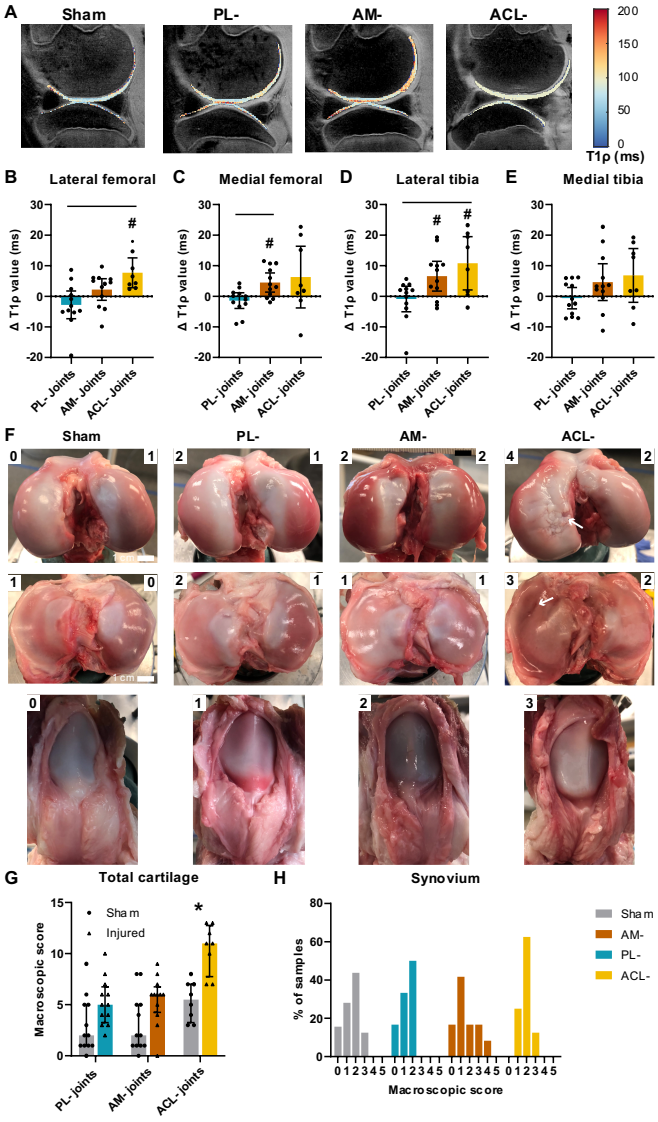

Fig. 3. Cartilage degeneration and synovium inflammation. (A) Representative sagittal MR images overlayed with T1ρ maps of articular cartilage. Interlimb differences in T1ρ value for (B) lateral femoral, (C) medial femoral, (D) lateral tibial, and (E) medial tibial articular cartilage. #P<0.05 compared to 0 from one sample t-test; bars indicate P<0.05 between injury type, from one-way ANOVA with Tukey post hoc test or Welch ANOVA with Dunnett post hoc test for data sets with unequal variance. (F) Representative images of articular cartilage and synovium, with macroscopic scores shown in the corner of each image. White arrows indicate cartilage erosions to subchondral bone. (G) Composite macroscopic OARSI scores summed from the four articular cartilage compartments. *P<0.05 compared contralateral controls from Wilcoxon matched-pairs test. (H) Histogram of macroscopic OARSI scores for synovium, presented as a percent of samples for each group. Individual data points (n=12 for PL- and AM- groups, n=8 for ACL- group) presented with mean ± 95% CI (B-E) or median ± IQR (G).

Meniscus and collateral ligaments

The biomechanical effect of injury on the menisci and collateral ligaments of the knee joint was assessed by measuring the in-situ load carried by each tissue under the applied loading conditions. The load carried in the medial meniscus under applied anterior drawer was 33% greater for AM- joints and 3.7-fold greater for ACL- joints compared to contralateral joints (P≤0.029 for each) (Fig. 4A), while no significant differences were measured under applied compression (Fig. 4B). The load carried in the lateral meniscus was greater compared to contralateral joints for AM- joints under applied anterior drawer (by 2.7-fold, P=0.025, Fig. 4C) and for ACL- joints under applied compression (by 2.1-fold, P=0.045, Fig. 4D). No differences in meniscal loads were measured in PL- joints relative to contralateral controls. Next, the volume

212 of the menisci were measured from MRI (Fig. 4D) and compared between injured and control
213 joints. The medial and lateral menisci were 11% and 7% larger in AM- joints and 28% and 30%
214 larger in ACL- joints, respectively ($P \leq 0.048$ for all, Fig. 4F-G). No changes in meniscal size
215 were measured in PL- joints. For ACL- joints, in addition to the measurable increases in size, the
216 menisci qualitatively developed an oblique shape, and medial menisci developed an unorganized
217 fibrous posterior outgrowth, evident macroscopically and on MRI (Fig. S4). Overall, both in-situ
218 loading and volume of the menisci showed no change in PL- joints, moderate increases in AM-
219 joints, and substantial increases in ACL- joints.

220 In the medial and lateral collateral ligaments (MCL and LCL, respectively), the in-situ
221 load under applied anterior drawer was greater compared to contralateral controls for only ACL-
222 joints (79N vs. 2.5N for MCL and 11.7N vs. 1.1N for LCL on average for the ACL- and
223 contralateral joints, respectively), indicating that the collateral ligaments may play a large role in
224 stabilizing the knee only after complete ACL injury ($P \leq 0.0080$, Fig. S5A and B). The CSA of the
225 MCL only was significantly larger compared to contralateral controls in ACL- joints ($P=0.048$,
226 Fig. S5C and D). Therefore, the collateral ligaments greater loads and remodeled by increasing
227 in CSA in ACL- joints but not AM- or PL- joints.

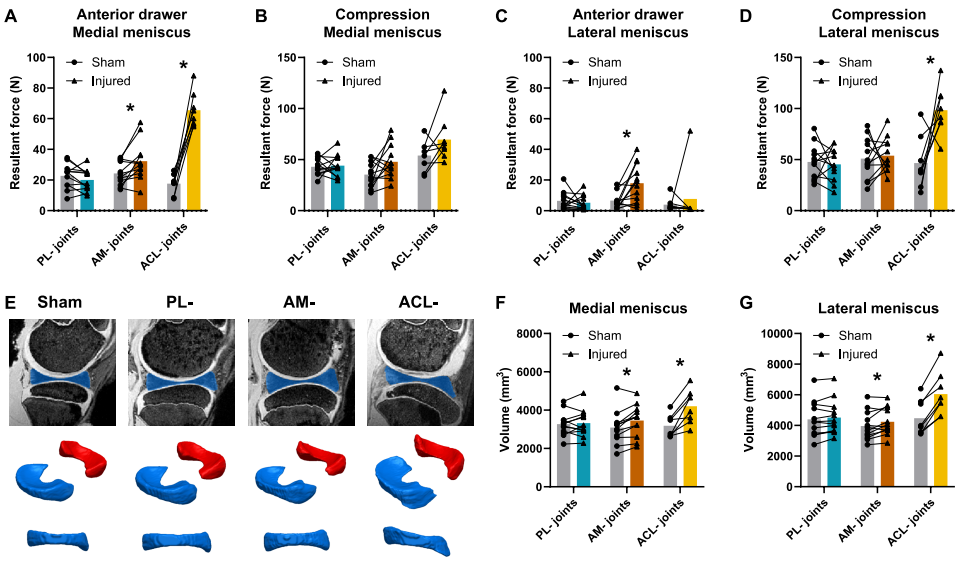

Fig. 4. Changes in meniscal loading and size after partial and complete ACL transection. In-situ forces in the medial meniscus under applied (A) anterior drawer and (B) axial compression. In-situ forces in the lateral meniscus under applied (C) anterior drawer and (D) axial compression. (E) Representative 3D models of menisci from each injury group, generated from MRI scans. Medial menisci shown in blue, lateral menisci in red. Volume of the (F) medial meniscus and (G) lateral meniscus. Lines connect paired joints. *P<0.05 between injured and contralateral, from paired t-test with Holm-Sidak correction. Individual data points (n=12 for PL- and AM- groups, n=8 for ACL- group) presented with mean.

Extension to adolescent animals

To investigate whether findings were similar for partial injuries in different ages during skeletal growth, AM and PL bundle injuries were created in a small subset of adolescent (6-month-old) pigs. Joint biomechanics, cartilage health, and meniscus volume were evaluated after 24 weeks. Interlimb differences in joint laxity were similarly elevated for AM- joints under AP drawer (P<0.05) in the adolescent injury group compared to the juvenile injury group, with no

244 significant difference in laxity for the PL- group (Fig. 5A, Fig. S6A). Laxity results were also
245 similar between the two age groups under applied axial compression and varus-valgus torque
246 (Fig. S6B and C). Cartilage T1ρ values appeared similarly elevated in femoral compartments of
247 AM- joints but not PL- joints, though significance was not reached (Fig. 5B and Fig. S6G-J).
248 Median composite macroscopic cartilage scores of injured joints trended higher in the adolescent
249 group, compared to the juvenile group, though differences were insignificant (Fig. 5C, Fig. S6F).
250 Lastly, the interlimb differences in medial and lateral meniscus volume were elevated, but not
251 statistically significant in the adolescent age group, with similar means between AM- and PL-
252 groups (Fig. 5D and E, Fig. S6D and E).
253

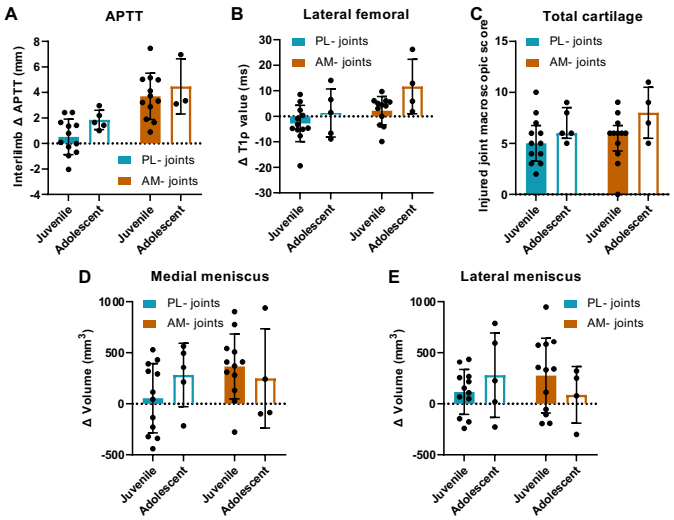

254

255 **Fig. 5. Joint laxity and cartilage T1ρ data for partial injuries created in adolescent (6-**
256 **month) compared to juvenile (3-month) pigs.** (A) Interlimb differences in APTT under applied
257 AP drawer. (B) Interlimb differences in T1ρ value for lateral femoral articular cartilage. (C)
258 Interlimb differences in macroscopic cartilage. Interlimb difference in volume of the (D) medial
259 and (E) lateral meniscus. Individual data points (n=5 for PL- and n=4 for AM- adolescent

260 groups, n=12 for PL- and AM- juvenile groups) presented with mean ± 95% CI (A,B,D,E) or
261 median ± IQR (C).
262
263 **Clinical Implications and Associations**
264 To place the observed degenerative outcomes in a clinically relevant framework,
265 specimens were grouped by equivalent Lachman test grade (Fig. 6A-D), which is a common
266 clinical exam to assess joint stability after ACL injury. Generally, mean side-side differences in
267 cartilage T1ρ values (P=0.0058), macroscopic cartilage scores (P=0.16), and medial (P=0.0003)
268 and lateral (P<0.0001) meniscus volume increased progressively for increasing Lachman test
269 grades. Significant interlimb differences were measured for cartilage T1ρ values and
270 macroscopic scores only for specimens with Lachman test grade D (P≤0.0086 for each), but
271 significant increases in medial and lateral meniscus volume were measured for specimens with
272 grade B as well as grade D (P≤0.012 for each). The lack of statistically significant findings for
273 grade C could be related to the limited sample size for this grade (n=4). Linear regressions were
274 performed to further investigate associations between joint stability and degeneration. Interlimb
275 differences in joint laxity were significantly associated with interlimb differences in cartilage
276 T1ρ values, macroscopic cartilage scores, and meniscal volume across all injury types (r^2=0.11-
277 0.79, P≤0.035 each) (Fig. S7, Fig. S8). Within injury type, significant associations were
278 measured for the AM- group (Figs. 8E-G, Fig. S8), specifically for macroscopic cartilage score
279 (r^2=0.37, P=0.036) and medial meniscus volume (r^2=0.45, P=0.016). Such associations were not
280 observed for either the PL- or ACL- groups. Pooling all injury types, these findings indicate that
281 joint destabilization is positively associated with the extent of joint degradation. For AM bundle

injuries that range from Lachman grades A to C, this linear association with joint stability is even clearer.

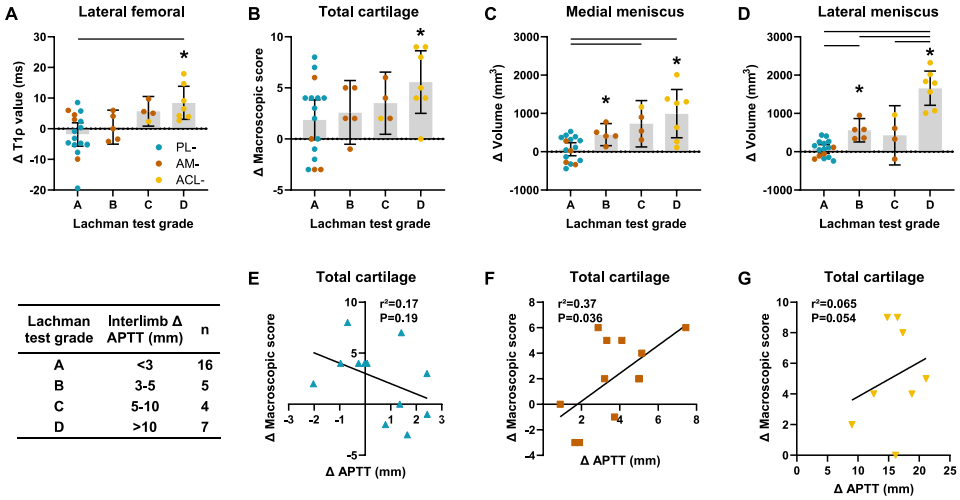

Lachman test grade	Interlimb Δ APTT (mm)	n
A	<3	16
B	3-5	5
C	5-10	4
D	>10	7

Fig. 6. Degenerative outcomes as a function of changes in laxity. Interlimb difference in (A) lateral femoral joint cartilage T1ρ, (B) composite macroscopic cartilage score, (C) medial meniscus volume and (D) lateral meniscus volume, grouped by the equivalent Lachman test grade from applied anterior-posterior drawer in biomechanical testing. *P<0.05 compared to 0 from one sample t-test; bars indicate P<0.05 between injury type, from one-way ANOVA with Tukey post hoc test. Continuous plots of interlimb difference in macroscopic cartilage score versus interlimb difference in APTT for the (E) PL- group, (F) AM- group, and (G) ACL- group. Statistical results from linear regression analyses shown in graph. Individual data points (n=12 for PL- and AM- groups, n=8 for ACL- group) presented with mean ± 95% CI (A-D).

DISCUSSION

There is presently a lack of data to inform clinical treatment of partial ACL injury in young patients, and large exploratory clinical studies are difficult to perform in this patient population. The present study provides a comprehensive analysis of functional and degenerative

299 changes in the knee joint after partial (isolated AM or PL bundle) and complete ACL injury in
300 skeletally immature subjects using a preclinical porcine model and clinically relevant outcome
301 measures. Our results indicate that ACL injury severity (partial or complete) impacts outcomes,
302 and equally importantly, that partial injury location (AM or PL bundle) also impacts outcomes.
303 Relatedly, the degree of degenerative changes was associated with the extent of joint
304 destabilization. Joint laxity increases were minimal for PL bundle injury, minor for AM bundle
305 injury, and major for ACL injury. In both partial injury cases, the remaining bundle remodeled
306 through an increase in CSA to attempt to restore ACL function and stabilize the knee joint.
307 Cartilage degeneration and meniscal hypertrophy were observed to a minor degree after AM
308 bundle injury and to a major degree after ACL injury, but not after PL bundle injury. Generally,
309 sex did not impact degenerative outcomes.

310 The joint laxity findings in this study are consistent with studies in humans, which report
311 minor (0-6 mm) increases in laxity after partial ACL tears (*7, 11, 13, 16*) compared to major (6-
312 12 mm) increases in laxity after complete ACL tears (*7, 11*). ACL injuries are commonly
313 diagnosed on the field or in the office through physical examination using a Lachman test, which
314 assesses tibial translation under anterior loads, or a pivot shift test, which evaluates tibial
315 subluxation under compressive and rotational loads (*25*). Therefore, the small differences in
316 laxity for partial ACL injuries point to challenges in diagnosis, particularly for PL bundle tears.
317 This is supported by a clinical study in adults which found that 50% of partial tears confirmed
318 through arthroscopy were diagnosed as a false negative using an arthrometer designed to
319 quantify joint laxity (*26*). In the current study, no significant difference in side-to-side laxity was
320 measured under anterior or rotational loads for the PL bundle injury group. In fact, all specimens
321 from the PL bundle injury group fell within the Lachman grade A (indicative of a "normal"

322 joint), suggesting that many of these injuries may go undiagnosed and untreated. Imaging,
323 primarily MRI, can add value as a complementary diagnostic tool in cases where physical
324 examination is inconclusive. Therefore, physical exams paired with MRI appear to be the best
325 current process for diagnosing partial ACL tears, although there remains space for improvement
326 of diagnostic sensitivity and specificity (*11, 27*). Diagnostic accuracy has the potential for
327 improvement through implementing higher resolution MRI protocols or newer sequences
328 capable of better contrast for ligaments (*28*). There also remains the potential for development of
329 new clinical exams which can detect partial injuries.

330 Our functional data is consistent with clinical studies in adults which reported that a
331 greater number of PL bundle injuries were biomechanically functional than AM bundle injuries
332 (*11*). Data is less definitive in pediatric patients, since currently only two studies evaluate
333 outcomes after partial injury in young patients (*13, 16*). Kocher et al. found patients with a PL
334 bundle injury were more likely to require a subsequent surgery (*16*), which is contradictory to
335 findings in this study. However, survivor bias may be a source for this discrepancy. In that study,
336 patients with Lachman grade C or D underwent surgical reconstruction and were not included,
337 which would exclude more AM bundle injuries than PL bundle injury based on our laxity
338 findings. Additionally, it is possible that a greater percentage of AM bundle tears progress to
339 complete ACL tears before receiving treatment. Human clinical practice may gauge the need for
340 surgery by progression from partial to complete tear, but this idea may need to be reconsidered,
341 since our data shows that degenerative changes can occur after partial ACL injury with joint
342 instability even without progression to a complete tear. Moreover, the lack of degenerative
343 changes in partial ACL injury with little joint instability could provide a rationale for non-
344 operative treatment, allowing more growth to occur prior to surgical intervention if needed.

345 Our findings are consistent with preclinical in-vivo studies of partial ACL injury as well.
346 A study in skeletally mature sheep found gross and histological cartilage degradation and
347 meniscal damage 40 weeks after AM bundle injury (*29*). Another study in skeletally mature
348 rabbits found histological evidence of meniscal degeneration 8 weeks after both AM and PL
349 bundle injuries (*30*). Although factors including skeletal maturity and time from injury differ
350 between these studies and our study, the consistent findings show that partial ACL injury alone
351 leads to long-term joint degeneration across different preclinical small and large animal models.
352 Furthermore, our study extends these prior findings to show that degeneration occurs even in the
353 context of skeletally immature joints, despite the potential for higher healing/remodeling
354 capacity.

355 Interestingly, the cartilage degeneration that we measured macroscopically and from MRI
356 did not necessarily correspond to one another, particularly in the AM bundle injured group which
357 showed significantly elevated cartilage T1ρ values but little macroscopic cartilage damage.
358 These two metrics inherently measure different outcomes, since macroscopic scoring reflects
359 large structural damage and loss of tissue, while T1ρ values reflects cartilage matrix
360 proteoglycan content of existing tissue. While elevated T1ρ values are often used as an early
361 predictor of future degeneration (*31*), macroscopic scoring reflects later-stage structural
362 degeneration. These two metrics may capture different phases of degeneration, and we would
363 predict that macroscopic scores for the AM bundle injury group would be increased for a longer
364 follow-up timepoint.

365 In addition to cartilage, changes in the meniscus were also associated with joint
366 instability, suggesting meniscal hypertrophy may be an early indicator of joint degeneration. This
367 is supported by data from a guineapig model, where meniscal hypertrophy was tied to cartilage

368 damage after ACL injury (*32*). Although little to no data exist regarding meniscal size changes
369 after ACL injury in humans, larger meniscus volume in middle-aged women was tied to later
370 development of structural OA (*33*). While it is common to evaluate meniscal tears after ACL
371 injury, meniscal size, independent of the presence of injury, is often overlooked. However,
372 meniscus size may be an important indicator of overall joint health. Furthermore, meniscus size
373 may be a more repeatable metric across time and may not require specialized MRI sequences,
374 such as T1ρ.

375 This study has implications for treatment of partial ACL tears, since we showed
376 significant meniscal and chondral pathology after partial ACL injury at the equivalence of a
377 grade B or higher Lachman test. Although we saw differences in outcomes due to injury type, the
378 extent of destabilization may be a better metric as a basis for treatment, since we saw significant
379 associations between cartilage degeneration and joint laxity even within AM bundle injuries. Our
380 results suggest that surgical intervention may be appropriate for patients with Lachman grade B
381 or above, and more likely to be necessary in patients with an AM bundle tear rather than PL
382 bundle tear. Additionally, the increase in remaining bundle CSA with no change in T2* value
383 indicates that viable tissue capable of functional remodeling can remain after a partial ACL
384 injury. This points to advantages in surgical techniques which preserve the intact tissue. Single
385 bundle augmentation techniques which repair or reconstruct only the injured bundle are
386 relatively new but gaining in popularity (*34-38*). These techniques have the advantage of
387 preserving the functional remaining tissue and may cause less donor site morbidity since smaller
388 grafts would be required.

389 This study includes several limitations, including the use of an animal model. While the
390 pig is an established preclinical model for musculoskeletal studies (*19*) and the ACL bundles

391 function similarly between pigs and humans (*20*), there are some differences in knee anatomy
392 (*21*) and physiological loading compared to humans. Furthermore, human patients are prescribed
393 physical therapy and activity restrictions, while we did not attempt to restrict animal activity or
394 acquire metrics for physical activity. Moreover, our evaluation of joint stability does not account
395 for active stabilization provided by the muscles, so it is possible that the joint is more stable in-
396 vivo. Nevertheless, the degenerative changes we detected occurred in the presence of muscle
397 function in-vivo. Additionally, our surgical model of ACL injury does not account for damage to
398 other tissues that may occur during the high impact of a naturally occurring ACL injury.
399 However, our model does isolate the effects of progressive degeneration caused by the loss of
400 joint stability. The injured bundle or entire ACL was removed in our surgical model. This
401 prevents any healing, which has been observed in a limited capacity in clinical cases (*39*). An
402 additional limitation includes the use of contralateral limbs as a control. These may differ from
403 joints in healthy animals due to altered gait or limb compensation after injury of the ipsilateral
404 joint. Lastly, the conclusions in this study are limited to only one timepoint after injury and do
405 not capture the time course of degenerative changes. Future longitudinal studies to assess the
406 progression of the degenerative outcomes would be useful for distinguishing early predictors of
407 degeneration and identifying an ideal window for implementing treatment interventions to
408 prevent degenerative changes.

409 This study fills key gaps in knowledge about degenerative changes after partial ACL
410 injury in skeletally immature subjects. We leverage a large animal model to collect detailed data
411 about joint biomechanics, tissue remodeling, and cartilage degeneration which are not possible to
412 collect in clinical studies. Our data show that the extent of destabilization after an ACL injury
413 may serve as a predictor of degeneration, irrespective of the injury type (partial or complete) or

414 partial injury location (AM or PL bundle). Associations in this study also imply that there may
415 not be a key threshold beyond which degenerative changes occur, but instead, a continuous
416 gradient where even small increases in laxity can cause minor degeneration. Overall, this study
417 provides a fundamental basis for informing clinical treatments in young patients with partial
418 ACL tears.
419

420 **MATERIALS AND METHODS**

421 **Study design**

422 The objective of this study was to evaluate the outcomes of partial ACL injury as a
423 function of tear location (AM or PL bundle), with covariates of sex and age, in a skeletally
424 immature surgical porcine model. All animals were bred at the North Carolina State University
425 Swine Educational Unit, and all experimental protocols were approved by the North Carolina
426 State University Institutional Animal Care and Use Committee. Sample sizes were calculated
427 using a power analysis described in the "Statistical analysis" section. A total of 32 juvenile
428 Yorkshire crossbreed pigs (age: 13 ± 1 week, weight: 34 ± 5 kg) underwent unilateral
429 arthroscopic transection of the AM bundle (n=6 female, n=6 male), the PL bundle (n=6 female,
430 n=6 male), or the complete ACL (n=4 female, n=4 male) with a sham operation performed on
431 the contralateral joint. Injury type and injured limb side were randomized. To confirm findings in
432 an older age group, a small subset of 9 adolescent pigs (age: 25 ± 1 week, weight: 129 ± 21 kg)
433 underwent unilateral arthroscopic transection of the AM bundle (n=3 female, n=1 male) or PL
434 bundle (n=4 female, n=1 male). One adolescent animal which was meant to undergo AM bundle
435 transection was excluded due to a pre-existing partial ACL tear to the PL bundle. The endpoint
436 was set at 24 weeks to experimentally evaluate joint biomechanics, cartilage health, and

437 remodeling of soft tissues in the knee joint. Data were collected and analyses were performed in
438 a blinded manner, where possible. No outliers were excluded in the presented data.
439
440 **Surgical procedure**
441 Prior to surgery, all pigs were sedated and received analgesics and antimicrobials.
442 Operations were performed arthroscopically (Arthrex Synergy System) under general anesthesia.
443 The knee joints were accessed through medial and lateral parapatellar incisions (~0.5 cm long).
444 The infrapatellar fat pad was partially removed using a 3.5 mm motorized shaver (SabreTooth,
445 Arthrex) to visualize the ACL. A freer elevator was inserted between the AM and PL bundles
446 near the tibial insertion and used to bluntly separate the bundles. A triangle knife (Ectra II Knife
447 4448, Smith & Nephew) was inserted into the separation and (1) turned anteriorly to transect the
448 AM bundle, (2) turned posteriorly to transect the PL bundle, or (3) used to transect the full cross-
449 section of the ACL. The remnant of the transected bundle or complete ligament was debrided
450 using a shaver to ensure loss of function and prevent healing. In the contralateral sham-operated
451 control limb, the infrapatellar pad was similarly partially removed. The ACL bundles were
452 separated with a freer elevator but not transected. Following the operation, skin incisions were
453 suture closed, a local analgesic was administered through subcutaneous injection at the portal
454 sites, and the joint was covered with an antimicrobial adhesive drape. Animals were given
455 analgesics and antimicrobials for 3 days post-operatively. Animals were allowed full weight
456 bearing immediately following surgery and housed in pens with no restriction of movement.
457 After 6 months (23.9 ± 0.3 weeks), all animals were euthanized, and hind limbs were collected.
458 Skin and excess muscle were removed, and knee joints were wrapped in saline-soaked pads and
459 stored at -20 °C.

460

461 **Magnetic resonance imaging**

462 Prior to scanning, joints were thawed. Joints were imaged at full extension. Imaging was
463 performed using a Siemens Magnetom Prisma 3T MRI system and a knee coil. Joints were
464 scanned using a T1ρ fast low-angle shot (FLASH) sequence (FOV: 128x128x84mm, voxel size:
465 0.4x0.4x1.5mm, FA: 10°, TR: 8.74ms, TE: 4.60ms, spin-lock frequency: 500 Hz, TSL: 0, 10, 20,
466 30, 40ms) and a T2 susceptibility weighted imaging (SWI) sequence (FOV: 160x160x128mm,
467 voxel size: 0.4x0.4x0.8mm, FA: 12°, TR: 31.0ms, TE: 3.3,7.1,11.4,15.7,20.0,24.4ms). Following
468 scanning, joints were stored at -20 °C for subsequent biomechanical testing. T1ρ and T2*
469 relaxation maps were created by fitting monoexponential decay function on a voxel-by-voxel
470 basis to the 5 spin-lock times and 6 echo times, respectively, using a custom MATLAB script.

471 Articular cartilage from the medial and lateral condyles of the femur and tibia were
472 manually segmented by a single user from T1ρ images with 0 ms spin-lock time using
473 commercial software (Simpleware ScanIP). Using a MATLAB script, the segmented areas were
474 transposed onto T1ρ relaxation maps described above, and the median T1ρ relaxation time was
475 calculated for each of the four segmented cartilage compartments.

476 Similarly, the AM bundle, PL bundle, complete ACL, MCL, LCL, and medial and lateral
477 menisci were manually segmented by a single user from T2* images with 15.7ms echo time. The
478 median T2* relaxation time was calculated for each ACL bundle. Additionally, the volume of
479 each segmented tissue was recorded, and the cross-sectional area (CSA) of the AM and PL
480 bundles, the complete ACL, MCL, and LCL were calculated as previously described (*17, 18*).
481 Briefly, each segmented tissue was exported as a surface mesh, and analyzed using a MATLAB
482 script. Each mesh was rotated such that a line of best fit through the mesh vertices aligned with

483 the z-axis. The CSA was calculated for slices of the mesh in 1 mm increments along the z-axis,
484 then averaged over the middle 50% of slices.
485
486 **Biomechanical testing**
487 Biomechanics of the knee (stifle) joint were evaluated using a 6 degree-of-freedom
488 (DOF) robotic testing system (KR300 R2500, KRC4, Kuka) equipped with a universal force-
489 moment sensor (Omega160 IP65, ATI Industrial Automation), and integrated through the
490 simVitro software knee module (Cleveland Clinic). To prepare for testing, joints were thawed at
491 room temperature and trimmed to expose the femoral and tibial diaphyses. The femoral head and
492 the distal end of the tibia were removed using a bone saw, then bones were fixed using
493 fiberglass-reinforced epoxy (Everglass, Evercoat) in molds designed to fit in custom clamps for
494 testing. Joints were again stored at -20 °C and thawed at room temperature one day prior to robot
495 testing.
496 The femoral end of the joint was fixed to a rigid testing platform, while the tibial end was
497 fixed to the robotic system at 40° of flexion. A 3D digitizer (G2X MicroScribe) was used to
498 determine an anatomic coordinate system. Joints were sprayed with saline and lightly wrapped in
499 a pad throughout testing to maintain hydration. A passive flexion path was determined by flexing
500 the joint from 40° to 90° while minimizing forces/moments in the remaining 5 DOFs. Then,
501 loads/torques were separately applied to the tibia in the anterior-posterior (AP) (100 N), proximal
502 (axial compression, 140 N), and VV (5 Nm) directions/rotations at 60° of joint flexion while
503 recording kinematic paths. Kinematics were then replayed while recording forces. Next, the joint
504 capsule was removed, and kinematics were replayed while recording forces. The difference in
505 forces measured between the intact and capsule-deficient condition was calculated as the force

506 carried by the joint capsule, by the principle of superposition. This process was repeated after
507 transection of the AM bundle (or any remnant), PL bundle (or any remnant), MCL, LCL, PCL,
508 medial meniscus, lateral meniscus, medial femoral condyle, and lateral femoral condyle. Joint
509 laxity was measured by anterior-posterior tibial translation (APTT) under AP drawer, anterior
510 tibial translation (ATT) under axial compression, and VV rotation under VV moments. Load-
511 transformation curves were plotted for each loading condition using data points collected at
512 intervals of 20% of the maximum applied load.
513

514 **Macroscopic scoring**

515 During robotic testing and tissue dissection, gross images were taken of the synovium
516 following joint capsule dissection, as well as the femoral and tibial articular cartilage, following
517 removal of all other tissues, during robotic testing. Synovium and cartilage were macroscopically
518 scored using Osteoarthritis Research Society International (OARSI) guidelines for sheep and
519 goat (*24*). Although are no scoring guidelines for pigs, this scoring system has been used to
520 evaluate cartilage in previous porcine studies (*40, 41*). Synovial pathology was scored from 0
521 (normal) to 5 (severe), and articular cartilage of medial and lateral condyles of the femur and
522 tibia were scored from 0 (normal) to 4 (large erosions down to subchondral bone) by two blinded
523 reviewers. Disagreements between users were re-examined to determine a consensus. Scores
524 from the four cartilage compartments were added to give a total joint score.
525

526 **Statistical analyses**

527 Sample sizes were determined using a power analysis based on prior work that
528 demonstrated the ability of transection of the AM bundle and ACL in cadaveric joints to generate

529 different levels of initial joint instability (*42*). Using an overall α level of 0.05 (accounting for
530 multiple comparisons), a power of 0.8, and an effect size of 1.5 for the AM- group, a sample size
531 of n=12 was selected to measure a difference between injured and sham-operated joints. For
532 complete loss of ACL function, much larger effect sizes are expected (>3), so a sample size of
533 n=8 was used for this group.

534 Normality of all data sets was confirmed using Shapiro-Wilk test, and equal variance
535 between data sets was tested using Brown-Forsythe test. Joint kinematics, tissue forces under
536 applied loads, tissue size metrics, and bundle T2* values were compared between injured and
537 sham-operated joints using paired t-tests with Holm-Sidak's correction for multiple comparisons.
538 Interlimb differences in joint kinematics and cartilage T1ρ were compared between injury types
539 using a one-way ANOVA with Tukey's post hoc comparison and compared to zero with one
540 sample t-tests. Interlimb differences in macroscopic and histologic cartilage scores were
541 compared to zero using one sample Wilcoxon test and between injury groups using a Kruskal
542 Wallis test. For data sets with unequal variance, Welch ANOVA with Dunnett post hoc
543 comparison was used. To evaluate clinically relevant outcomes, samples were grouped into
544 equivalent Lachman test grades according to IKDC guidelines (A: <3 mm, B: 3-5 mm, C: 5-10
545 mm, D: >10 mm) (*43*), based on joint translations under AP drawer. Interlimb differences in
546 cartilage T1ρ, macroscopic cartilage scores, and meniscal volume were compared between
547 Lachman grades using one-way ANOVA and compared to zero with one sample t-test.
548 Associations were assessed between interlimb differences in APTT and interlimb differences in
549 cartilage scores and meniscal volume using linear regression across all injury types and within
550 injury types. All statistical analyses were performed in Prism (GraphPad), with overall
551 significance set at α=0.05 for all analyses with corrections for multiple comparisons done as

552 needed. Adjusted P values are reported. Data presented as mean ± 95% CI, unless stated
553 otherwise, and data are reported in supplemental material.
554

555 **References and Notes**

556 1. G. Kolata, in *The New York Times*. (2017), chap. D, pp. 1.
557 2. T. L. Sanders, H. Maradit Kremers, A. J. Bryan, D. R. Larson, D. L. Dahm, B. A. Levy,
558 M. J. Stuart, A. J. Krych, Incidence of Anterior Cruciate Ligament Tears and
559 Reconstruction: A 21-Year Population-Based Study. *Am J Sports Med* **44**, 1502-1507
560 (2016).
561 3. N. A. Mall, P. N. Chalmers, M. Moric, M. J. Tanaka, B. J. Cole, B. R. Bach, Jr., G. A.
562 Paletta, Jr., Incidence and trends of anterior cruciate ligament reconstruction in the
563 United States. *Am J Sports Med* **42**, 2363-2370 (2014).
564 4. B. C. Werner, S. Yang, A. M. Looney, F. W. Gwathmey, Jr., Trends in Pediatric and
565 Adolescent Anterior Cruciate Ligament Injury and Reconstruction. *J Pediatr Orthop* **36**,
566 447-452 (2016).
567 5. D. Zbrojkiewicz, C. Vertullo, J. E. Grayson, Increasing rates of anterior cruciate ligament
568 reconstruction in young Australians, 2000-2015. *Med J Aust* **208**, 354-358 (2018).
569 6. E. R. Dodwell, L. E. Lamont, D. W. Green, T. J. Pan, R. G. Marx, S. Lyman, 20 years of
570 pediatric anterior cruciate ligament reconstruction in New York State. *Am J Sports Med*
571 **42**, 675-680 (2014).
572 7. D. M. Daniel, M. L. Stone, R. Sachs, L. Malcom, Instrumented measurement of anterior
573 knee laxity in patients with acute anterior cruciate ligament disruption. *Am J Sports Med*
574 **13**, 401-407 (1985).

575 8. I. Kawashima, H. Hiraiwa, S. Ishizuka, R. Kawai, Y. Kusaka, K. Ohtomo, T. Tsukahara,
576 Incidence of Medial and Lateral Meniscal Tears After Delayed Anterior Cruciate
577 Ligament Reconstruction in Pediatric Patients. *Orthop J Sports Med* **8**,
578 2325967120964603 (2020).
579 9. C. L. Ardern, G. Ekas, H. Grindem, H. Moksnes, A. Anderson, F. Chotel, M. Cohen, M.
580 Forssblad, T. J. Ganley, J. A. Feller, J. Karlsson, M. S. Kocher, R. F. LaPrade, M.
581 McNamee, B. Mandelbaum, L. Micheli, N. Mohtadi, B. Reider, J. Roe, R. Seil, R.
582 Siebold, H. J. Silvers-Granelli, T. Soligard, E. Witvrouw, L. Engebretsen, 2018
583 International Olympic Committee consensus statement on prevention, diagnosis and
584 management of paediatric anterior cruciate ligament (ACL) injuries. *Knee Surg Sports*
585 *Traumatol Arthrosc*, (2018).
586 10. P. Colombet, D. Dejour, J. C. Panisset, R. Siebold, S. French Arthroscopy, Current
587 concept of partial anterior cruciate ligament ruptures. *Orthop Traumatol Surg Res* **96**,
588 S109-118 (2010).
589 11. D. Dejour, P. G. Ntagiopoulos, P. R. Saggin, J. C. Panisset, The diagnostic value of
590 clinical tests, magnetic resonance imaging, and instrumented laxity in the differentiation
591 of complete versus partial anterior cruciate ligament tears. *Arthroscopy* **29**, 491-499
592 (2013).
593 12. E. R. Hunt, C. A. Jacobs, C. E. Conley, M. L. Ireland, D. L. Johnson, C. Lattermann,
594 Anterior cruciate ligament reconstruction reinitiates an inflammatory and
595 chondrodegenerative process in the knee joint. *J Orthop Res* **39**, 1281-1288 (2021).
596 13. J. M. Fayard, B. Sonnery-Cottet, G. Vrgoc, P. O'Loughlin, G. D. de Mont Marin, B.
597 Freychet, T. D. Vieira, M. Thaunat, Incidence and Risk Factors for a Partial Anterior

598 Cruciate Ligament Tear Progressing to a Complete Tear After Nonoperative Treatment in
599 Patients Younger Than 30 Years. *Orthop J Sports Med* **7**, 2325967119856624 (2019).
600 14. P. N. Chalmers, N. A. Mall, M. Moric, S. L. Sherman, G. P. Paletta, B. J. Cole, B. R.
601 Bach, Jr., Does ACL reconstruction alter natural history?: A systematic literature review
602 of long-term outcomes. *J Bone Joint Surg Am* **96**, 292-300 (2014).
603 15. M. Group, J. S. Everhart, M. H. Jones, S. Yalcin, E. K. Reinke, L. J. Huston, J. T.
604 Andrish, C. L. Cox, D. C. Flanigan, C. C. Kaeding, R. A. Magnussen, N. Obuchowski, R.
605 D. Parker, A. D. Pedroza, R. A. Sanders, C. S. Winalski, K. P. Spindler, The Clinical
606 Radiographic Incidence of Posttraumatic Osteoarthritis 10 Years After Anterior Cruciate
607 Ligament Reconstruction: Data From the MOON Nested Cohort. *Am J Sports Med* **49**,
608 1251-1261 (2021).
609 16. M. S. Kocher, L. J. Micheli, D. Zurakowski, A. Luke, Partial tears of the anterior cruciate
610 ligament in children and adolescents. *Am J Sports Med* **30**, 697-703 (2002).
611 17. S. G. Cone, E. P. Lambeth, H. Ru, L. A. Fordham, J. A. Piedrahita, J. T. Spang, M. B.
612 Fisher, Biomechanical Function and Size of the Anteromedial and Posterolateral Bundles
613 of the ACL Change Differently with Skeletal Growth in the Pig Model. *Clin Orthop*
614 *Relat Res* **477**, 2161-2174 (2019).
615 18. D. Howe, S. G. Cone, J. A. Piedrahita, B. Collins, L. A. Fordham, E. H. Griffith, J. T.
616 Spang, M. B. Fisher, Sex-specific biomechanics and morphology of the anterior cruciate
617 ligament during skeletal growth in a porcine model. *J Orthop Res*, (2021).
618 19. S. G. Cone, P. B. Warren, M. B. Fisher, Rise of the Pigs: Utilization of the Porcine Model
619 to Study Musculoskeletal Biomechanics and Tissue Engineering During Skeletal Growth.
620 *Tissue Eng Part C Methods* **23**, 763-780 (2017).

621 20. J. W. Xerogeanes, R. J. Fox, Y. Takeda, H. S. Kim, Y. Ishibashi, G. J. Carlin, S. L. Woo,
622 A functional comparison of animal anterior cruciate ligament models to the human
623 anterior cruciate ligament. *Ann Biomed Eng* **26**, 345-352 (1998).
624 21. B. L. Proffen, M. McElfresh, B. C. Fleming, M. M. Murray, A comparative anatomical
625 study of the human knee and six animal species. *Knee* **19**, 493-499 (2012).
626 22. R. R. Regatte, S. V. Akella, A. J. Wheaton, G. Lech, A. Borthakur, J. B. Kneeland, R.
627 Reddy, 3D-T1rho-relaxation mapping of articular cartilage: in vivo assessment of early
628 degenerative changes in symptomatic osteoarthritic subjects. *Acad Radiol* **11**, 741-749
629 (2004).
630 23. S. V. Akella, R. R. Regatte, A. J. Gougoutas, A. Borthakur, E. M. Shapiro, J. B.
631 Kneeland, J. S. Leigh, R. Reddy, Proteoglycan-induced changes in T1rho-relaxation of
632 articular cartilage at 4T. *Magn Reson Med* **46**, 419-423 (2001).
633 24. C. B. Little, M. M. Smith, M. A. Cake, R. A. Read, M. J. Murphy, F. P. Barry, The
634 OARSI histopathology initiative - recommendations for histological assessments of
635 osteoarthritis in sheep and goats. *Osteoarthritis Cartilage* **18 Suppl 3**, S80-92 (2010).
636 25. V. Musahl, I. D. Engler, E. M. Nazzal, J. F. Dalton, G. A. Lucidi, J. D. Hughes, S.
637 Zaffagnini, F. Della Villa, J. J. Irrgang, F. H. Fu, J. Karlsson, Current trends in the
638 anterior cruciate ligament part II: evaluation, surgical technique, prevention, and
639 rehabilitation. *Knee Surg Sports Traumatol Arthrosc* **30**, 34-51 (2022).
640 26. J. Isberg, E. Faxen, S. Brandsson, B. I. Eriksson, J. Karrholm, J. Karlsson, KT-1000
641 records smaller side-to-side differences than radiostereometric analysis before and after
642 an ACL reconstruction. *Knee Surg Sports Traumatol Arthrosc* **14**, 529-535 (2006).

643 27. P. Van Dyck, E. De Smet, J. Veryser, V. Lambrecht, J. L. Gielen, F. M. Vanhoenacker,
644 L. Dossche, P. M. Parizel, Partial tear of the anterior cruciate ligament of the knee: injury
645 patterns on MR imaging. *Knee Surg Sports Traumatol Arthrosc* **20**, 256-261 (2012).
646 28. N. C. Nacey, M. G. Geeslin, G. W. Miller, J. L. Pierce, Magnetic resonance imaging of
647 the knee: An overview and update of conventional and state of the art imaging. *J Magn*
648 *Reson Imaging* **45**, 1257-1275 (2017).
649 29. K. I. Barton, B. J. Heard, J. L. Sevick, C. R. Martin, S. M. M. Shekarforoush, M. Chung,
650 Y. Achari, C. B. Frank, N. G. Shrive, D. A. Hart, Posttraumatic Osteoarthritis
651 Development and Progression in an Ovine Model of Partial Anterior Cruciate Ligament
652 Transection and Effect of Repeated Intra-articular Methylprednisolone Acetate Injections
653 on Early Disease. *Am J Sports Med* **46**, 1596-1605 (2018).
654 30. D. Wang, Z. Wang, M. Li, S. Xu, The underlying mechanism of partial anterior cruciate
655 ligament injuries to the meniscus degeneration of knee joint in rabbit models. *J Orthop*
656 *Surg Res* **15**, 428 (2020).
657 31. H. F. Atkinson, T. B. Birmingham, R. F. Moyer, D. Yacoub, L. E. Kanko, D. M. Bryant,
658 J. D. Thiessen, R. T. Thompson, MRI T2 and T1rho relaxation in patients at risk for knee
659 osteoarthritis: a systematic review and meta-analysis. *BMC Musculoskelet Disord* **20**, 182
660 (2019).
661 32. G. Du, H. Zhan, D. Ding, S. Wang, X. Wei, F. Wei, J. Zhang, B. Bilgen, A. M. Reginato,
662 B. C. Fleming, J. Deng, L. Wei, Abnormal Mechanical Loading Induces Cartilage
663 Degeneration by Accelerating Meniscus Hypertrophy and Mineralization After ACL
664 Injuries In Vivo. *Am J Sports Med* **44**, 652-663 (2016).

665 33. D. Xu, J. van der Voet, J. H. Waarsing, E. H. Oei, S. Klein, M. Englund, F. Zhang, S.
666 Bierma-Zeinstra, J. Runhaar, Are changes in meniscus volume and extrusion associated
667 to knee osteoarthritis development? A structural equation model. *Osteoarthritis Cartilage*
668 **29**, 1426-1431 (2021).
669 34. B. Sonnery-Cottet, R. Zayni, J. Conteduca, P. Archbold, T. Prost, Y. Carrillon, J. Clechet,
670 M. Thaunat, Posterolateral Bundle Reconstruction With Anteromedial Bundle Remnant
671 Preservation in ACL Tears: Clinical and MRI Evaluation of 39 Patients With 24-Month
672 Follow-up. *Orthop J Sports Med* **1**, 2325967113501624 (2013).
673 35. N. Shohat, D. Lindner, E. Tamir, Y. Beer, G. Agar, Prospective Comparison between
674 Remnant-Preserving Augmentation and Double-Bundle Reconstruction in Anterior
675 Cruciate Ligament Tears. *Isr Med Assoc J* **19**, 355-359 (2017).
676 36. A. M. Gipsman, N. Trasolini, G. F. R. Hatch, 3rd, Primary Anterior Cruciate Ligament
677 Single-Bundle Repair With Augmentation for a Partial Anterior Cruciate Ligament Tear.
678 *Arthrosc Tech* **7**, e367-e372 (2018).
679 37. G. Y. Ahn, T. H. Lee, K. J. Lee, S. Woo, Comparison of clinical outcomes and second-
680 look arthroscopic evaluations between anterior cruciate ligament anteromedial bundle
681 augmentation and single-bundle anterior cruciate ligament reconstruction. *Knee Surg*
682 *Relat Res* **32**, 45 (2020).
683 38. T. Tajima, N. Yamaguchi, Y. Morita, T. Yokoe, M. Nagasawa, T. Ota, S. Kawagoe, Y.
684 Nakamura, E. Chosa, Remnant-Preserved Single-Bundle Anterior Cruciate Ligament
685 Augmentation in Multi-ligamentous Knee Reconstruction. *J Knee Surg*, (2022).

686 39. E. H. Crain, D. C. Fithian, E. W. Paxton, W. F. Luetzow, Variation in anterior cruciate
687 ligament scar pattern: does the scar pattern affect anterior laxity in anterior cruciate
688 ligament-deficient knees? *Arthroscopy* **21**, 19-24 (2005).
689 40. N. P. Karamchedu, M. M. Murray, J. T. Sieker, B. L. Proffen, G. Portilla, M. Q. Costa, J.
690 Molino, B. C. Fleming, Bridge-Enhanced Anterior Cruciate Ligament Repair Leads to
691 Greater Limb Asymmetry and Less Cartilage Damage Than Untreated ACL Transection
692 or ACL Reconstruction in the Porcine Model. *Am J Sports Med* **49**, 667-674 (2021).
693 41. M. P. Pinette, J. Molino, B. L. Proffen, M. M. Murray, B. C. Fleming, Effects of Male
694 and Female Sex on the Development of Posttraumatic Osteoarthritis in the Porcine Knee
695 After Anterior Cruciate Ligament Surgery. *Am J Sports Med*, 3635465221102118 (2022).
696 42. D. Howe, S. G. Cone, J. A. Piedrahita, J. T. Spang, M. B. Fisher, Age and Sex-Specific
697 Joint Biomechanics in Response to Partial and Complete ACL Injury in the Porcine
698 Model. *J Athl Train*, (2021).
699 43. E. P. Mulligan, D. Q. McGuffie, K. Coyner, M. Khazzam, The reliability and diagnostic
700 accuracy of assessing the translation endpoint during the lachman test. *Int J Sports Phys*
701 *Ther* **10**, 52-61 (2015).
702

703 **Acknowledgments:** We would like to thank Laboratory Animal Resources (NC State) and the
704 Biomedical Research Imaging Center (UNC-CH) for their contributions to this work.
705 **Funding:**
706 National Institutes of Health grant F31AR077997 (DH)
707 National Institutes of Health grant R01AR071985 (MBF, EHG, LVS, JTS)
708 National Science Foundation grant DGE-1746939 (JDT)

Author contributions:

Conceptualization: DH, LVS, JTS, MBF

Methodology: DH, JDT, SDT, EHG, LVS, JTS, MBF

Investigation: DH, JDT, OB, SDT, LVS, JTS, MBF

Formal analysis: DH, JDT, SDT, EHG, MBF

Data Curation: DH, SDT

Visualization: DH

Funding acquisition: DH, JDT, LVS, JTS, MBF

Project administration: DH, MBF

Supervision: MBF

Writing – original draft: DH

Writing – review & editing: DH, JDT, OB, SDT, EHG, LVS, JTS, MBF

Competing interests: Authors declare that they have no competing interests.

Data and materials availability: All data are available in the main text or the supplementary materials.

SUPPLEMENTAL MATERIAL

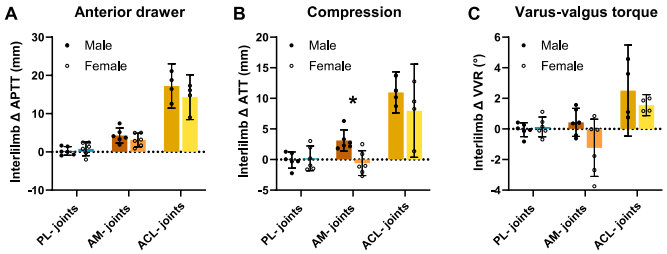

Figure S1. Sex-specific biomechanical outcomes. Interlimb differences in (A) anterior-posterior tibial translation (APTT) under applied AP drawer, (B) anterior tibial translation (ATT) under applied axial compression, and (C) varus-valgus (VV) rotation under applied VV moments. * P<0.05 between male and female, from one-way ANOVA with Tukey post hoc test. Individual data points presented with mean ± 95% CI.

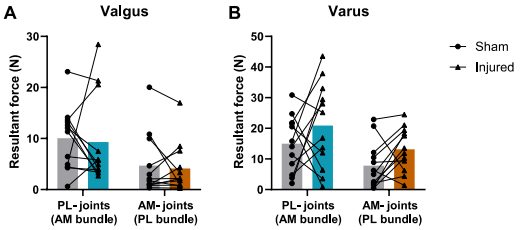

Figure S2. In-situ bundle forces under rotational loads. Resultant force in the uninjured bundle under applied (A) valgus moments and (B) varus moments. Lines connect paired joints. Individual data points presented with mean.

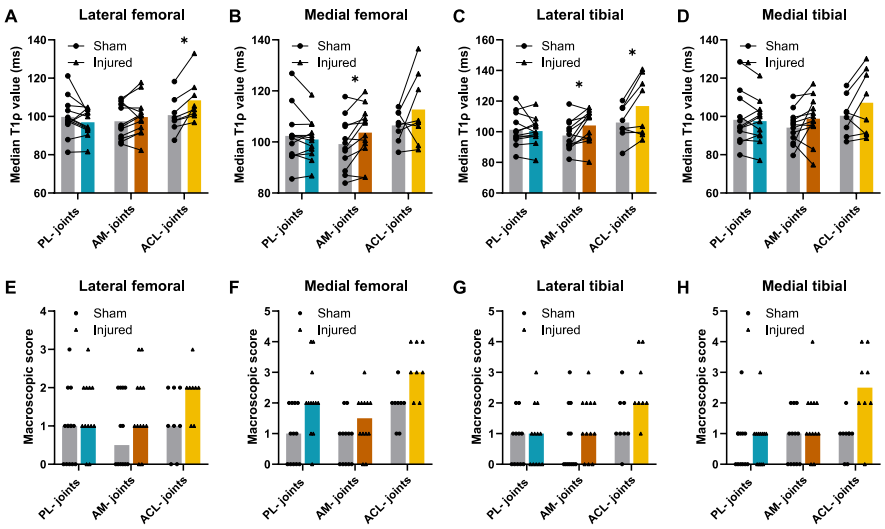

Figure S3. T1ρ values and macroscopic scores of cartilage compartments. T1ρ values of the (A) lateral femoral, (B) lateral tibial, (C) medial femoral, and (D) medial tibial cartilage compartments. Macroscopic OARSI score of the (E) lateral femoral, (F) lateral tibial, (G) medial femoral, and (H) medial tibial cartilage compartments. *P<0.05 between injured and contralateral, from paired t-test with Holm-Sidak correction. Individual data points presented with mean with lines connecting paired joints (A-D) or median ± IQR (E-H).

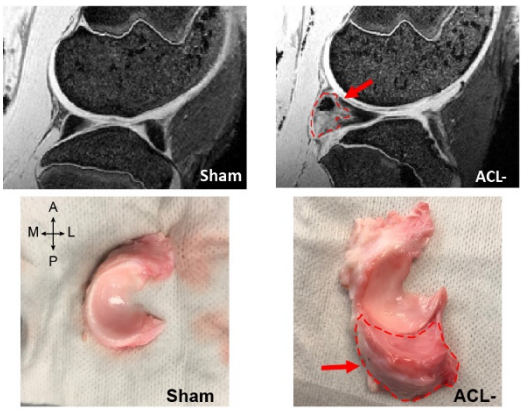

Figure S4. MRI and macroscopic images of medial menisci from sham-operated and ACL- joints. Red dotted lines indicate degenerative, fibrous outgrowth. Anterior-posterior and medial-lateral directions indicated.

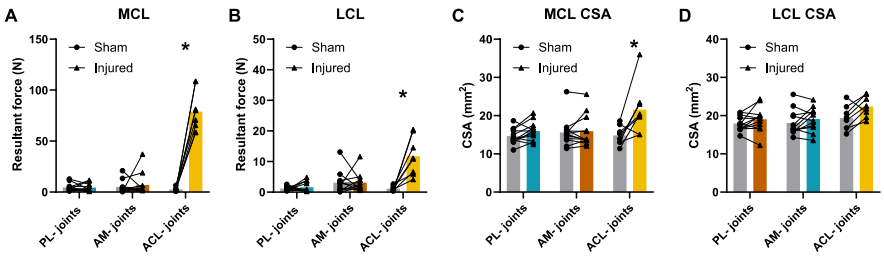

Figure S5. Collateral ligament remodeling after partial and complete ACL transection. In-situ forces in the (A) MCL and (B) LCL under applied anterior drawer. CSA of the (C) MCL and (D) LCL. Lines connect paired joints. *P<0.05 between injured and contralateral, from paired t-test with Holm-Sidak correction. Individual data points (n=12 for PL- and AM- groups, n=8 for ACL- group) presented with mean.

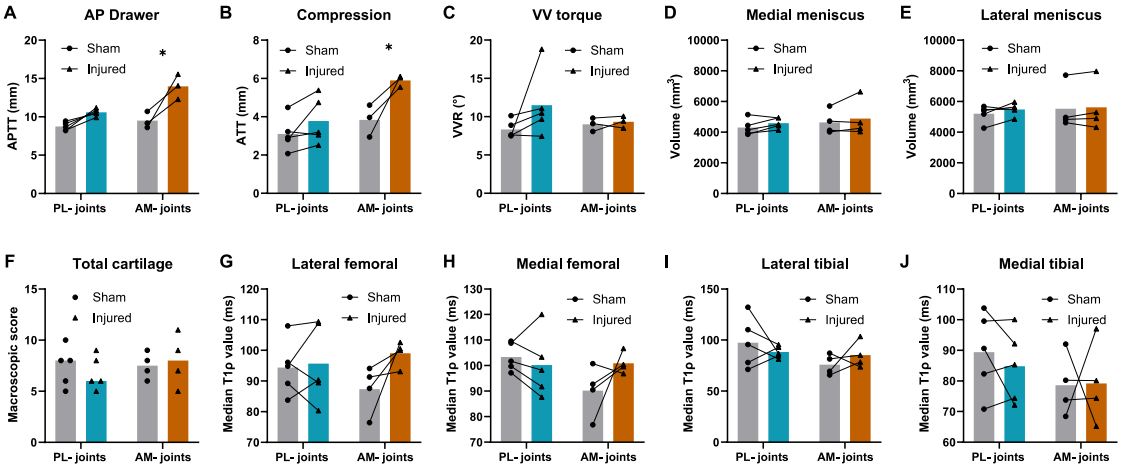

Figure S6. Biomechanical and degenerative outcomes after partial injuries created in adolescent (6 month) pigs. (A) APTT under applied AP drawer, (B) ATT under applied axial compression, and (C) VV rotation under applied VV moments. Volume of the (D) medial meniscus and (E) lateral meniscus. (F) Composite macroscopic OARSI scores summed from the four articular cartilage compartments. T1ρ value for (G) lateral femoral, (H) medial femoral, (I) lateral tibial, and (J) medial tibial articular cartilage. Lines connect paired joints. *P<0.05

between injured and contralateral, from paired t-test with Holm-Sidak correction. Individual data points (n=5 for PL- and n=4 for AM- groups) presented with mean.

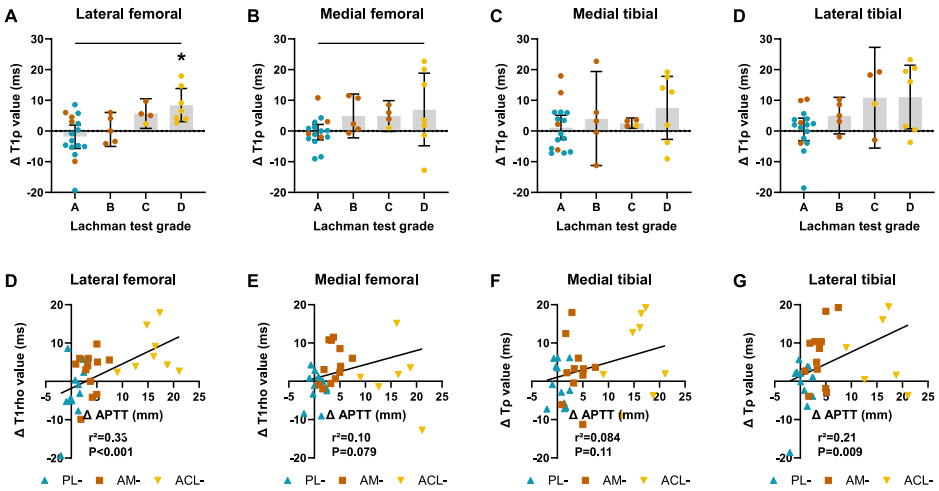

Figure S7. Interlimb difference in (A) lateral femoral, (B) medial femoral, (C) medial tibial, and (D) lateral tibial cartilage T1ρ value, grouped by the equivalent Lachman test grade. *P<0.05 compared to 0 from one sample t-test; bars indicate P<0.05 between injury type, from one-way ANOVA with Tukey post hoc test. Continuous plots of interlimb difference in (E) lateral femoral, (F) medial femoral, (G) medial tibial, and (H) lateral tibial cartilage T1ρ value versus interlimb difference in APTT across all injury groups. Statistical results from linear regression analyses shown in graph. Individual data points presented with mean ± 95% CI (A-D).

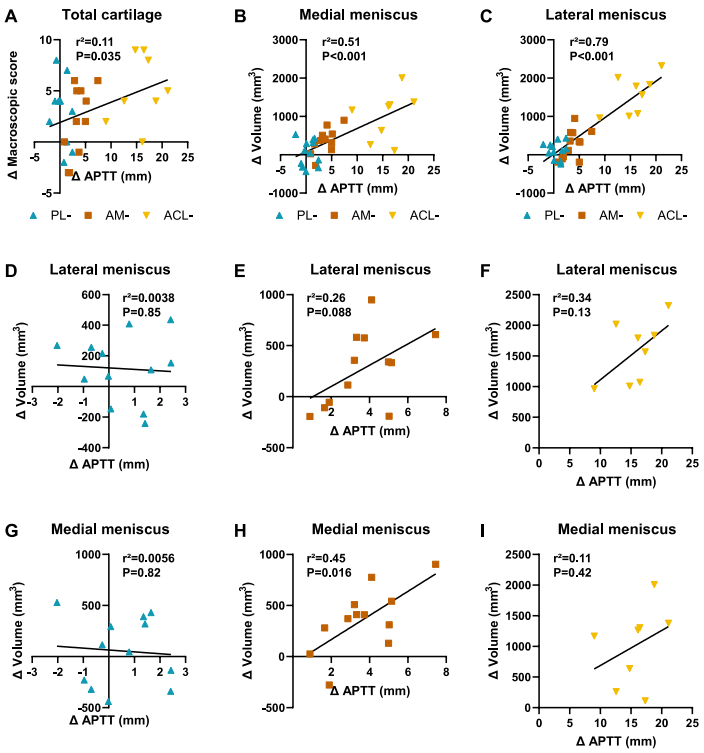

Figure S8. Interlimb difference in (A) composite macroscopic cartilage score, (B) medial meniscus volume and (C) lateral meniscus volume versus interlimb difference in APTT across all injury groups. Interlimb difference in medial meniscus volume versus interlimb difference in APTT for the (D) PL- group, (E) AM- group, and (F) ACL- group. Interlimb difference in lateral meniscus volume versus interlimb difference in APTT for the (G) PL- group, (H) AM- group, and (I) ACL- group. Statistical results from linear regression analyses shown in graph.